

Supplementary Information

Highly Bioresistant, Hydrophilic and Rigidly Linked Trityl-nitroxide Biradicals for Cellular High-field Dynamic Nuclear Polarization

Ru Yao,^{a,#} David Beriashvili,^{b,#} Wenxiao Zhang,^a Shuai Li,^a Adil Safeer,^b Andrei Gurinov,^b Antal Rockenbauer,^c Yin Yang,^d
Yuguang Song,^a Marc Baldus*^b and Yangping Liu*^a

-
- [a] The province and ministry co-sponsored collaborative innovation center for medical epigenetics, Tianjin Key Laboratory on Technologies Enabling Development of Clinical Therapeutics and Diagnostics, School of Pharmacy, Tianjin Medical University, Tianjin 300070, P. R. China.
Email: liyuyangping@tmu.edu.cn
- [b] NMR Spectroscopy group, Bijvoet Center for Biomolecular Research, Utrecht University, Padualaan 8, 3584 CH Utrecht, The Netherlands.
Email: m.baldus@uu.nl
- [c] Institute of Materials and Environmental Chemistry, Hungarian Academy of Sciences and, Department of Physics, Budapest University of Technology and Economics, Budafoki ut 8, 1111 Budapest, Hungary.
- [d] State Key Laboratory of Elemento-organic Chemistry, Collaborative Innovation Center of Chemical Science and Engineering, Nankai University, Tianjin 300071, China.

Equal first author contribution.

Table of Contents

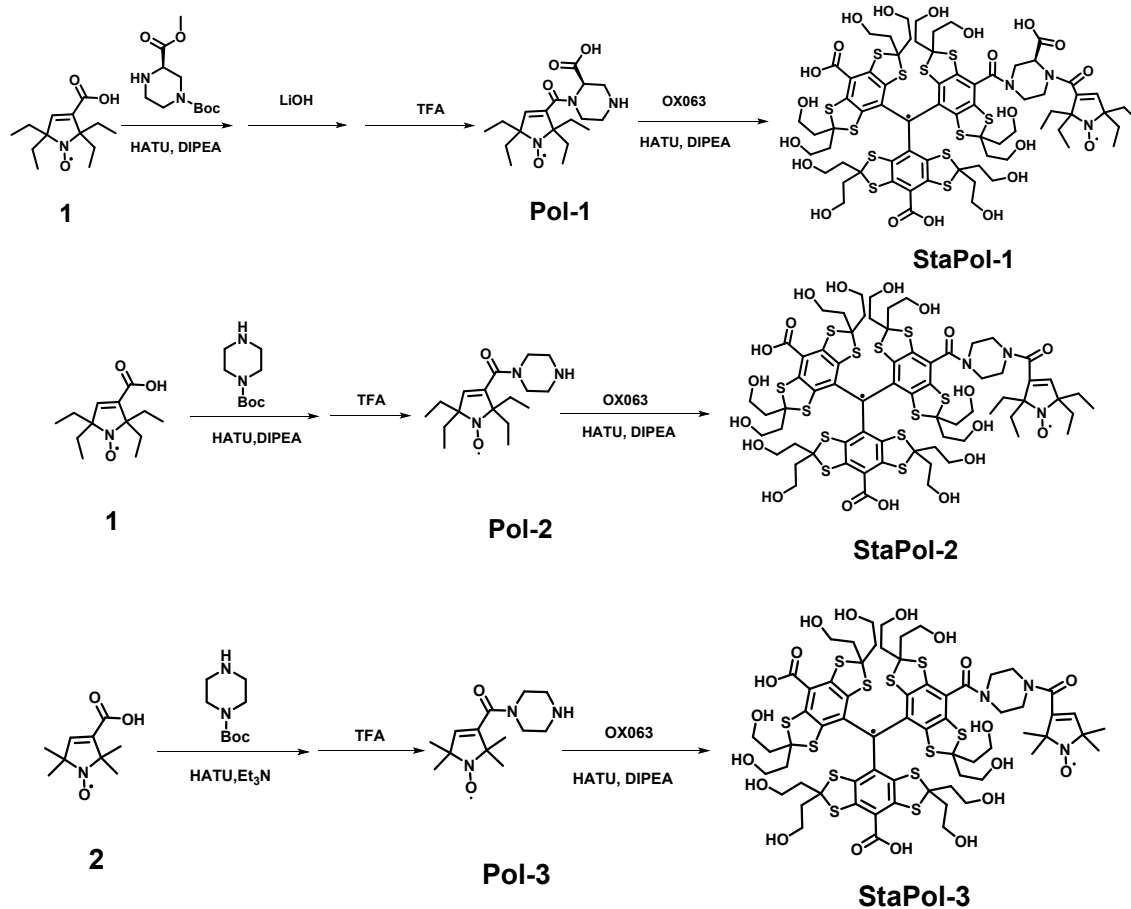
1. Synthetic procedures of StaPols and H-StaPols	S3
2. EPR experiments and spectral simulation of H-StaPols and H-SNAPol-1	S5
<i>Experimental and simulated X-band EPR spectra at room temperature</i>	S5
<i>Experimental and simulated X-band EPR spectra at low temperature</i>	S6
3. EPR experiments and spectral simulation of TN biradicals	S6
<i>Experimental and simulated X-band EPR spectra at room temperature</i>	S7
<i>Experimental and simulated Q-band EPR spectra at room temperature</i>	S7
<i>Experimental and simulated X-band EPR spectra at low temperature</i>	S8
4. Characterization of StaPols and H-StaPols	S9
<i>HPLC chromatograms of StaPols</i>	S9
<i>HRMS spectra of StaPols, H-StaPols, H-SNAPol-1 and their intermediates</i>	S9
5. Reduction of biradicals with ascorbic acid or in the cell lysates	S14
<i>Reduction of biradicals with ascorbic acid</i>	S15
<i>Reduction of biradicals in HeLa cell lysates</i>	S17
6. Solid-state NMR DNP experiments	S20
7. Materials and methods for solid-state NMR DNP experiments	S26

Experimental Procedures

1. Synthetic procedures of StaPols

General materials and methods

Dichloromethane (CH_2Cl_2) was redistilled with CaH_2 and dimethylformamide (DMF) was passed through a column of molecular sieves. (S)-1-N-Boc-piperazine-3-carboxylic acid methyl ester, lithium hydroxide, 1-Boc-piperazine, N,N,N-Triethylamine (Et_3N), 2-(7-Azabenzotriazol-1-yl)-N,N,N',N'-tetramethyluronium hexafluorophosphate (HATU), N,N-diisopropylethyl-amine (DIPEA), trifluoroacetic acid (TFA) were purchased and used without further purification. 2,2,5,5-Tetramethyl-3-pyrroline-1-oxyl-3-carboxylic acid (Compound **2**)¹, 2,2,5,5-tetraethyl-3-pyrroline-1-oxyl-3-carboxylic acid (Compound **1**)² and **OX063**³ was prepared according to the previously reported methods. H-StaPols were obtained according to the previously reported methods.⁴ Thin layer chromatography analysis was performed on glass 0.25 mm silica gel plates which were visualized by exposure to UV light. Flash column chromatography was employed using silica gel with 200-300 mesh. High-resolution mass spectrometry was carried out employing electrospray ionization methods (ESI) for the end products and LTQ Orbitrap discovery (ESI, Thermofisher scientific) for the reaction intermediates. Analytical HPLC was done on an Agilent 1100 instrument equipped with a G1315B DAD detector and G1311A pump, and data are shown in Fig. S1. Semipreparative HPLC was carried out on SSI 1500 equipped with a UV/Vis detector and versa-pump.



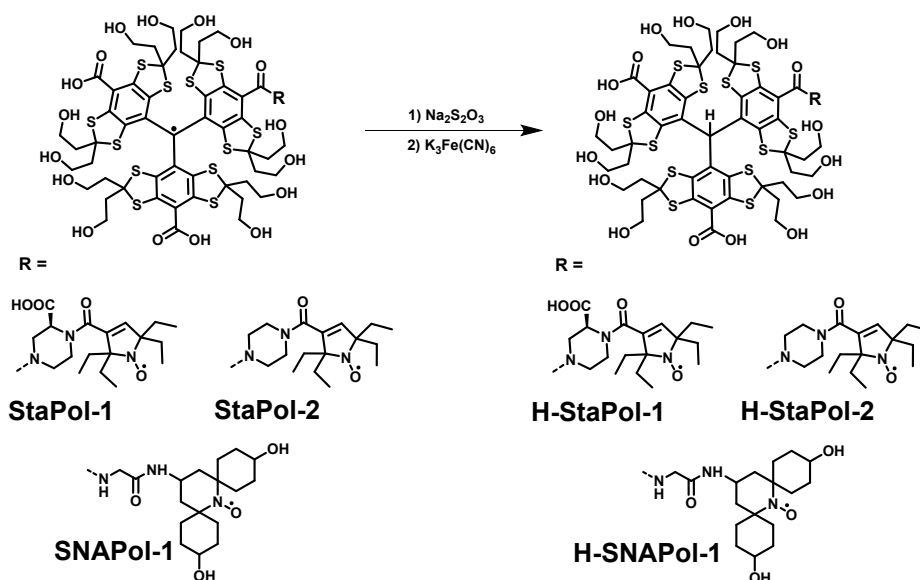


Fig. S1 Synthesis of StaPols, H-StaPols and H-SNAPol-1.

Pol-1

To a solution of 2,2,5,5-tetraethyl-3-pyrroline-1-oxyl-3-carboxylic acid (Compound **1**, 24 mg, 0.099 mmol) and DIPEA (166 μL , 0.950 mmol) in DMF (2 mL) was dropwise added HATU (43.75 mg, 0.115 mmol) in DMF (0.5 mL). Then, (S)-1-N-Boc-piperazine-3-carboxylic acid methyl ester (31.2 mg, 0.128 mmol) in DMF (0.5 mL) was added, and the resulting yellow solution was stirred for 24 h at room temperature in the darkness. The reaction mixture was extracted with EtOAc (20 mL) and 1 M HCl (20 mL). The organic layer was separated, washed with brine (30 mL), dried over anhydrous sodium sulfate, filtered and concentrated in vacuo. The crude product was dissolved in DCM and purified by column chromatography on silica gel using DCM/ EtOAc (9:1) as an eluent to afford the methyl ester-containing nitroxide as a yellow solid. Then, lithium hydroxide (114 mg, 4.75 mmol) was added to the solution of the methyl ester-containing nitroxide (44.2 mg, 0.095 mmol) in MeOH/ H_2O (1:1). TLC was used to monitor the hydrolysis reaction. After completion of the reaction (~4 hours), the reaction mixture was extracted with EtOAc (20 mL) and 1 M HCl (20 mL). The organic layer was separated, washed with brine (20 mL), dried over anhydrous sodium sulfate, filtered and concentrated in vacuo. The resulting residue was redissolved in DCM (1 mL) and then trifluoroacetic acid (TFA, 1 mL) was added. The resulting solution was stirred at ambient temperature for 3 h. The solvent and TFA were completely removed under vacuum. **Pol-1** (20.9 mg, 60 % over three steps) was obtained as a red oil which was used without further purification. **Pol-1**, HRMS (ESI, m/z): calcd for $\text{C}_{18}\text{H}_{29}\text{N}_3\text{O}_4^-$ ($[\text{M}-\text{H}]^-$), 351.2164; found, 351.2165.

StaPol-1

To a solution of OX063 (26 mg, 0.019 mmol) and DIPEA (33.2 μL , 0.19 mmol) in DMF (2 mL) was dropwise added HATU (8.75 mg, 0.023 mmol) in DMF (0.5 mL). Then, Pol-1 (16.8 mg, 0.048 mmol) in DMF (0.5 mL) was added. After stirring overnight at room temperature, the reaction mixture was concentrated under vacuum. The resulting residue was redissolved in phosphate buffer (20 mM, pH 7.4) and separated by column chromatography on reversed-phase C18 using water followed by 0-25% MeOH in H_2O as eluents to afford a green solid (8 mg, 25 %). **StaPol-1**, HRMS (ESI, m/z): calculated for $\text{C}_{70}\text{H}_{89}\text{N}_3\text{O}_{21}\text{S}_{12}^{2-}$ ($[\text{M}-2\text{H}]^{2-}$) 845.6324; found, 845.6327.

Pol-2

To a solution of 2,2,5,5-tetraethyl-3-pyrroline-1-oxyl-3-carboxylic acid (Compound **1**, 24 mg, 0.099 mmol) and DIPEA (166 μL , 0.950 mmol) in DMF (2 mL) was dropwise added HATU (43.75 mg, 0.115 mmol) in DMF (0.5 mL). Then, 1-Boc-piperazine (23.8 mg, 0.128 mmol) in DMF (0.5 mL) was added, and the resulting yellow solution was stirred for 24 h at room temperature in the darkness. The reaction mixture was extracted with EtOAc (20 mL) and 1 M HCl (20 mL). The organic layer was separated, washed with brine (30 mL), dried over anhydrous sodium sulfate, filtered and concentrated in vacuo. The crude product was dissolved in DCM and purified by column chromatography on silica gel using DCM/ EtOAc (10:1) as an eluent to afford the precursor of **Pol-2** as a yellow solid. The precursor was redissolved in DCM (1 mL) and then trifluoroacetic acid (TFA, 1 mL) was added. The resulting solution was stirred at ambient temperature for 3 h. The solvent and TFA were completely removed under vacuum. **Pol-2** (21.3 mg, 80 % over two steps) was obtained as a red oil which was used without further purification. **Pol-2**, HRMS (ESI, m/z): calcd for $\text{C}_{17}\text{H}_{30}\text{N}_3\text{O}_2^{+}$ ($[\text{M}+\text{H}]^+$), 309.2416; found, 309.2408.

StaPol-2

To a solution of OX063 (26 mg, 0.019 mmol) and DIPEA (33.2 μ L, 0.19 mmol) in DMF (2 mL) was dropwise added HATU (8.75 mg, 0.023 mmol) in DMF (0.5 mL). Then, **Pol-2** (12 mg, 0.035 mmol) in DMF (0.5 mL) was added. After stirring overnight at room temperature, the reaction mixture was concentrated under vacuum. The resulting residue was redissolved in phosphate buffer (20 mM, pH 7.4) and separated by column chromatography on reversed-phase C18 using water followed by 0-30% MeOH in H₂O as eluents to afford a green solid (9 mg, 30 %). **StaPol-2**, HRMS (ESI, m/z): calculated for C₆₉H₈₉N₃O₁₉S₁₂^{••2-} ([M-2H]²⁻) 823.6375; found, 823.6324.

Pol-3

To a solution of 2,2,5,5-tetraethyl-3-pyrroline-1-oxyl-3-carboxylic acid (Compound **2**, 18 mg, 0.097 mmol) and DIPEA (166 μ L, 0.950 mmol) in DMF (2 mL) was dropwise added HATU (43.75 mg, 0.115 mmol) in DMF (0.5 mL). Then, 1-Boc-piperazine (23.8 mg, 0.128 mmol) in DMF (0.5 mL) was added, and the resulting yellow solution was stirred for 24 h at room temperature in the darkness. The reaction mixture was extracted with EtOAc (20 mL) and 1 M HCl (20 mL). The organic layer was separated, washed with brine (30 mL), dried over anhydrous sodium sulfate, filtered and concentrated in vacuo. The crude product was dissolved in DCM and purified by column chromatography on silica gel using DCM/ EtOAc (10:1) as an eluent to afford the precursor of **Pol-3** as a yellow solid. The precursor was redissolved in DCM (1 mL) and then trifluoroacetic acid (TFA, 1 mL) was added, the resulting solution was stirred at ambient temperature for 3 h. The solvent and TFA were completely removed under vacuum. **Pol-3** (19.5 mg, 80 % over two steps) was obtained as a red oil which was used without further purification. **Pol-3**, HRMS (ESI, m/z): calcd for C₁₃H₂₂N₃O₂^{•+} ([M+H]⁺), 253.1790; found, 253.1783.

StaPol-3

To a solution of OX063 (26 mg, 0.019 mmol) and DIPEA (33.2 μ L, 0.19 mmol) in DMF (2 mL) was dropwise added HATU (8.75 mg, 0.023 mmol) in DMF (0.5 mL). Then, **Pol-3** (13 mg, 0.048 mmol) in DMF (0.5 mL) was added. After stirring overnight at room temperature, the reaction mixture was concentrated under vacuum. The resulting residue was redissolved in phosphate buffer (20 mM, pH 7.4) and separated by column chromatography on reversed-phase C18 using water followed by 0-25% MeOH in H₂O as eluents to afford a green solid (12 mg, 40 %). **StaPol-3**, HRMS (ESI, m/z): calculated for C₆₅H₈₃N₃O₁₉S₁₂^{••-} ([M]⁻) 1593.2269; found, 1593.2201.

H-StaPols and H-SNAPol-1

To a 10 mL Schlenk bottle containing StaPol-1 (1.0 mg, 0.59 μ mol) and Na₂S₂O₄ (0.4 mg, 2.30 μ mol) was added 1 mL of degassed water under argon atmosphere. The reaction mixture was stirred at room temperature for 30 min and then concentrated under vacuum. The resulting residue was dissolved in water (1 mL) and K₃Fe(CN)₆ (0.75 mg, 2.30 μ mol) was added. After reacting at room temperature for 30 min, the solution was concentrated in vacuo. The resulting residue was redissolved in phosphate buffer (0.5 mL, 20 mM, pH 7.4) and then purified by reverse-phase semi-preparative HPLC to give a yellow solid **H-StaPol-1** in quantitative yield. **H-StaPol-1**, HRMS (ESI, m/z): calculated for C₇₀H₉₀N₃O₂₁S₁₂^{••-} ([M-2H]²⁻) 846.1363; found, 846.1335. Similarly, **H-StaPol-2** and **H-SNAPol-1** were also synthesized. **H-StaPol-2**, HRMS (ESI, m/z): calculated for C₆₉H₉₀N₃O₁₉S₁₂^{••2-} ([M-2H]²⁻) 824.1414; found, 824.1400. **H-SNAPol-1**, HRMS (ESI, m/z): calculated for C₆₉H₉₀N₃O₂₁S₁₂^{••2-} ([M-2H]²⁻) 840.1363; found, 840.1361.

2. X-Band EPR experiments and spectral simulation of H-StaPols and H-SNAPol-1

X-band EPR measurements at ~298 K and ~150 K were carried out in 50 μ L capillary on Bruker EMX-plus X-band spectrometer. General instrumental settings were as follows: modulation frequency, 100 kHz; microwave power, 10 mW; modulation amplitude, 1 G (~298 K) and 2 G (~150 K).

EPR spectral simulation was performed by the EPR/ROKI program which was developed by Professor Rockenbauer⁵. The reported g factor and hyperfine constant (A_N) of the corresponding nitroxides were used as initial parameters for spectral simulations.^{6, 7} EPR parameters obtained by the simulation were shown in Table S1 and S2, which were well consistent with the reported values.

All parameters were optimized simultaneously until the sum of squares of deviations between experimental and calculated spectra was minimized. Note that only the relative g-tensor values were provided since the frequency of the EPR instrument was not calibrated. The errors were estimated by fine-tuning only one of the parameters while the other parameters were kept constant. The errors were obtained once the sum of squares of deviations did not vary significantly with the parameter with a regression of usually $\geq 98.5\%$. The estimated errors for room-temperature EPR spectra were 0.0002 for g-factors, 0.15 G for A_N , 0.1 G for W, while the errors for low-temperature spectra were 0.0005 for g-factors, 1 G for A_N , 1 G for W.

2.1 Experimental and simulated X-band EPR spectra at room temperature

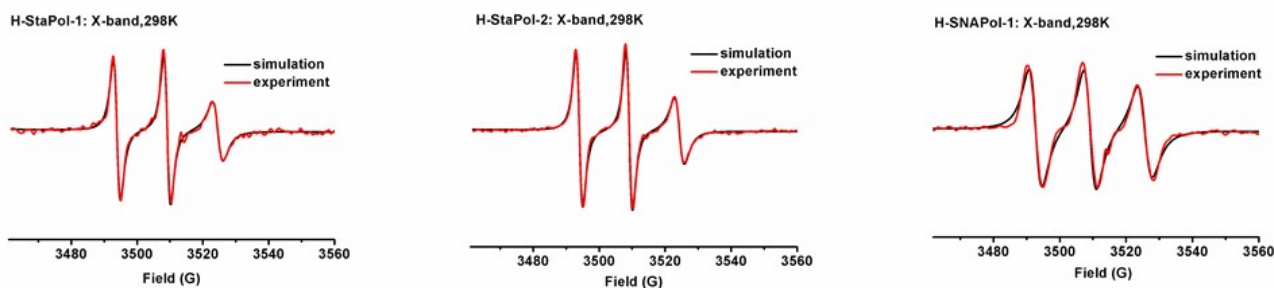


Fig. S2 X-band experimental (red line) and simulated (black line) EPR spectra of H-StaPols (100 μM) and H-SNAPol-1 (100 μM) in phosphate buffer (20 mM, pH 7.4) at room temperature (~ 298 K).

Table S1. EPR parameters of H-StaPols and H-SNAPol-1 at ~ 298 K.

	H-StaPol-1	H-StaPol-2	H-SNAPol-1
g_{NO}	2.0064	2.0064	2.0063
A_{N}/G	15.34	15.36	16.50
W/G	2.69	2.49	3.78

2.2 Experimental and simulated X-band EPR spectra at low temperature

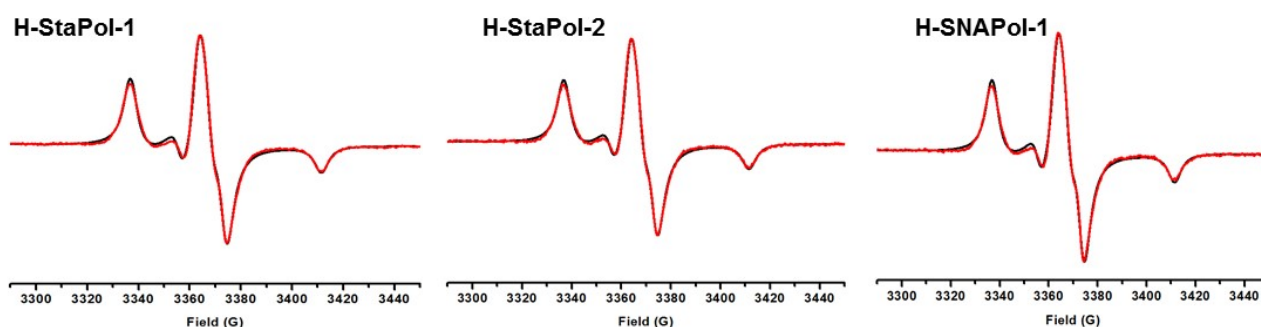


Fig. S3 X-band experimental (red line) and simulated (black line) EPR spectra of H-StaPols (100 μM) and H-SNAPol-1 (100 μM) in glycerol/water (60/40, v/v) at low temperature (~ 150 K).

Table S2. EPR parameters of H-StaPols (100 μM) and H-SNAPol-1 (100 μM) in glycerol/water (60/40, v/v) at ~ 150 K.

	H-StaPol-1	H-StaPol-2	H-SNAPol-1
g_{Nx}	2.0094	2.0095	2.0094
g_{Ny}	2.0069	2.0069	2.0069
g_{Nz}	2.0031	2.0031	2.0030
A_{Nx}	5.8	5.7	5.3
A_{Ny}	7.1	7.0	7.9
A_{Nz}	35.9	36.2	37.1
W/G	3.2	3.3	3.2

3. EPR experiments and spectral simulation of TN biradicals

X-band EPR measurements at ~ 298 K and ~ 150 K were carried out in 50 μL capillary on Bruker EMX-plus X-band spectrometer. General instrumental settings were as follows: modulation frequency, 100 kHz; microwave power, 10 mW;

modulation amplitude, 1 G (~298 K) and 2 G (~150 K).

Q-band CW spectra were collected at ~298 K on a Bruker E580 (34 GHz) spectrometer. General instrumental settings were as follows: modulation frequency, 50 kHz; microwave power, 3 mW; modulation amplitude, 0.1 G.

EPR simulation of liquid-state EPR spectra (both X-band and Q-band) of TN biradicals was performed by the EPR/ROKI program. The following spin Hamiltonian was used^{5, 8}:

$$H_{iso} = \hat{B} * \hat{g}_1 * \hat{S}_1 \cdot \mu_B + \hat{B} * \hat{g}_2 * \hat{S}_2 \cdot \mu_B + J \hat{S}_1 \hat{S}_2 + \hat{S}_1 * \hat{A}_1 * \hat{I}_1$$

In order to reduce the number of variables when we simulated the spectra of the biradicals, the isotropic g factor and the hyperfine constants of the corresponding nitroxides (See Table S1) were used as initial parameters for spectral simulations. Because the molecules can tumble freely and quickly at room temperature, anisotropies of the magnetic resonance parameters are averaged out. Accordingly, in the liquid state, ten non-linear parameters were adjusted in the simulation. The parameters were optimized simultaneously until the sum of the squares of the deviations between the experimental and calculated spectra was minimized. Table S3 shows five of the parameters (i.e., exchange interactions value, J ; g_{NO} and g_{Tri} ; the hyperfine constant of the nitrogen atom, A_N ; the line-width, W) obtained from simulation of X-band EPR spectra, which are more important than the others. Using the similar procedure for simulation of EPR spectra of H-StaPols (See above), the errors of the parameters for X-band EPR spectra were estimated: g-factors: 0.0002; A_N : 0.15 G; J : 2 G; W : 0.5 G. Table S4 showed the corresponding EPR parameters obtained from simulation of the Q-band EPR spectra with the estimated errors: g-factors: 0.0002; A_N : 0.2 G; J : 0.5 G; W : 0.5 G.

EPR simulation of Solid-state EPR spectra (X-band) of StaPol-1 and StaPol-2 was performed by the DNP/ROKI program. The spin Hamiltonian was used as given in our previous study^{5, 8}:

$$H_{SH} = \hat{B} * \hat{g}_1 * \hat{S}_1 \cdot \mu_B + \hat{B} * \hat{g}_2 * \hat{S}_2 \cdot \mu_B + J \hat{S}_1 \hat{S}_2 + D(2S_{z1}S_{z2} - S_{x1}S_{x2} - S_{y1}S_{y2}) + \hat{S}_1 * \hat{A}_1 * \hat{I}_1 + \hat{S}_2 * \hat{A}_2 * \hat{I}_2$$

The anisotropic values of g tensors (g_{Nx} , g_{Ny} , g_{Nz}) and hyperfine constants (A_{Nx} , A_{Ny} , A_{Nz}) obtained from simulation of X-band EPR spectra of H-StaPols at low temperature (See Table S2) were used as initial parameters for spectral simulations. For simulation of the solid-state EPR spectra of StaPol-1 and StaPol-2, 20 non-linear parameters in total were adjusted (18 for the biradical and two for the monomer). These parameters were optimized simultaneously until the sum of the squares of the deviations between the experimental and calculated spectra was minimized: anisotropy of the g_{NO} value: g_{Nx} , g_{Ny} , g_{Nz} ; anisotropy of the nitrogen hyperfine constant, A_N : A_{Nx} , A_{Ny} , A_{Nz} ; the isotropic g_{Tri} value; exchange and dipolar interactions value: J , D ; polar angles: X , Φ ; euler angles: α , β , γ ; the line-width, W . Table S5 showed 15 of the parameters which are more important than the others. The errors of the EPR parameters at low temperature were estimated: g-factors: 0.0005; A_N : 2 G; W : 0.5 G; J : 2 G; D : 2 G; polar and euler angles: 5 deg.

3.1 Experimental and simulated X-band EPR spectra at room temperature

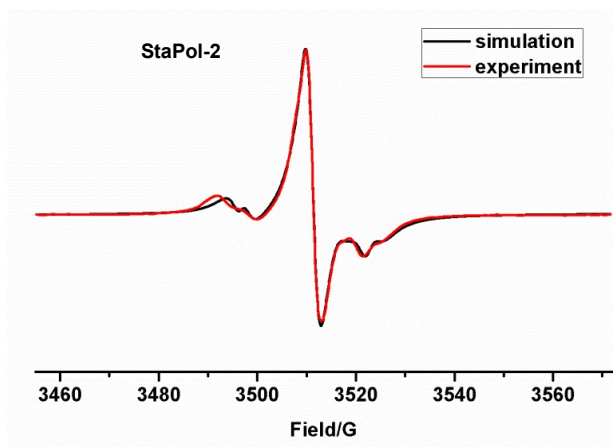
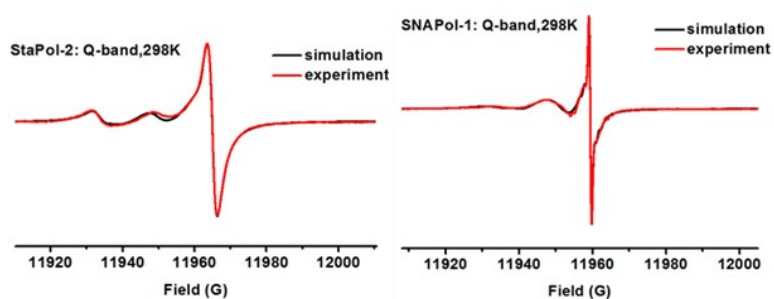


Fig. S4 X-band experimental (red line) and simulated (black line) EPR spectra of StaPol-2 (300 μ M) in phosphate buffer (20 mM, pH 7.4) at room temperature (~298 K).

Table S3. Magnetic parameters of StaPol-1 and StaPol-2 in the liquid state at ~298 K (X-band).

	StaPol-1	StaPol-2
J/G	14.6	11.2
g_{NO}	2.0050	2.0050
g_{Tri}	2.0034	2.0034
A_N/G	15.75	15.85
W/G	4.34	3.72

3.2 Experimental and simulated Q-band EPR spectra at room temperature**Fig. S5** Q-band experimental (red line) and simulated (black line) EPR spectra of StaPol-2 and SNAPol-1 (300 μ M) in phosphate buffer (20 mM, pH 7.4) at room temperature (~298 K).**Table S4.** Magnetic parameters of StaPol-1, StaPol-2 and SNAPol-1 in the liquid state at ~298 K (Q-band).

	StaPol-1	StaPol-2	SNAPol-1 ^[a,b]
J/G	10.5	7.9	29.1 ^[a] /4.0 ^[b]
g_{NO}	2.0047	2.0046	2.0047
g_{Tri}	2.0033	2.0034	2.0034
A_N/G	14.99	15.11	16.08
W/G	4.93	4.60	4.20

Two stable conformers were observed for SNAPol-1 at Q-band EPR ⁴: [a] conformer 1 (29%), [b] conformer 2 (71%).

3.3 Experimental and simulated X-band EPR spectra at low temperature

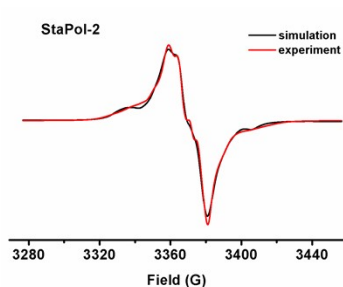


Fig. S6 X-band experimental (red line) and simulated (black line) EPR spectra of StaPol-2 (300 μM) in glycerol/water (60/40, v/v) at low temperature (~ 150 K).

Table S5. Magnetic parameters of StaPol-1 and StaPol-2 (300 μM) in glycerol/water (60/40, v/v) at ~ 150 K (X-band).

	StaPol-1	StaPol-2
g_{Nx}	2.0094	2.0100
g_{Ny}	2.0069	2.0061
g_{Nz}	2.0021	2.0020
A_{Nx}/G	4.2	3.7
A_{Ny}/G	6.9	5.6
A_{Nz}/G	31.0	28.3
g_{Tri}	2.0041	2.0041
J/G	23	21
D/G	9	8
X	175	174
Φ	12	-6
α	21	25
β	-31	-21
γ	8	8
W/G	4.90	4.67

4. Characterization of StaPols and H-StaPols

4.1 HPLC chromatograms of StaPols

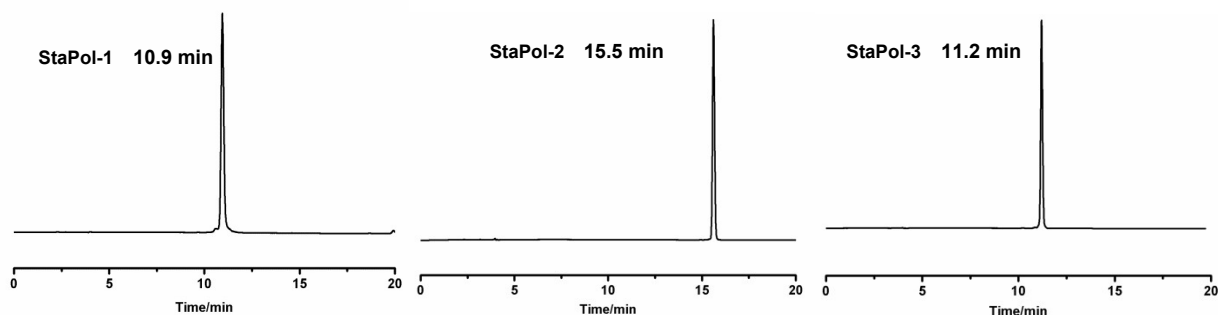


Fig. S7 The purity of the samples ranged from 97% to 99%. Samples were measured in $\text{CH}_3\text{CN}/\text{CH}_3\text{COONH}_4$ (20 mM), 10%-50%, 0-20 min, Flow speed: 1 mL/min. Column: Inertsil ODS-3.5 μm 4.6 x 250 mm. Column temperature: 25°C, UV detection at 464 nm.

4.2 HRMS spectra of StaPols, H-StaPols, H-SNAPol-1 and their intermediates

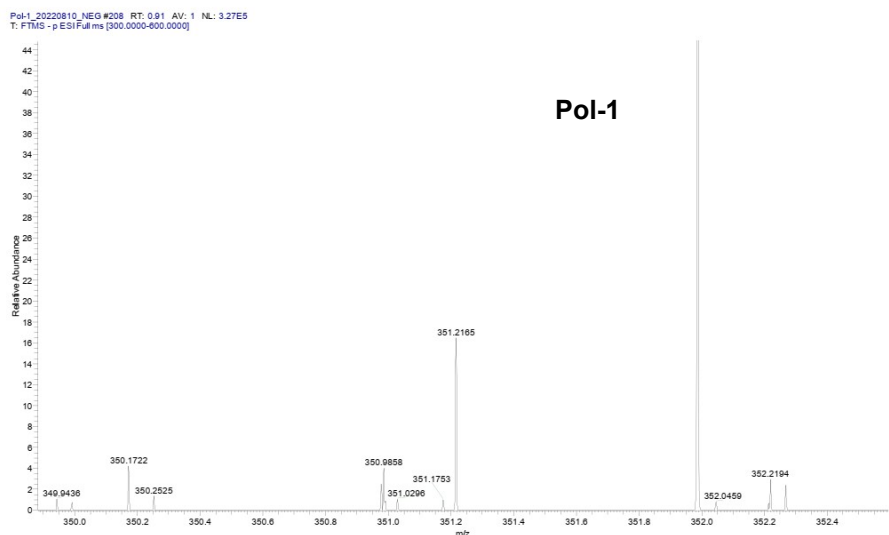


Fig. S8 HRMS spectrum of Pol-1.

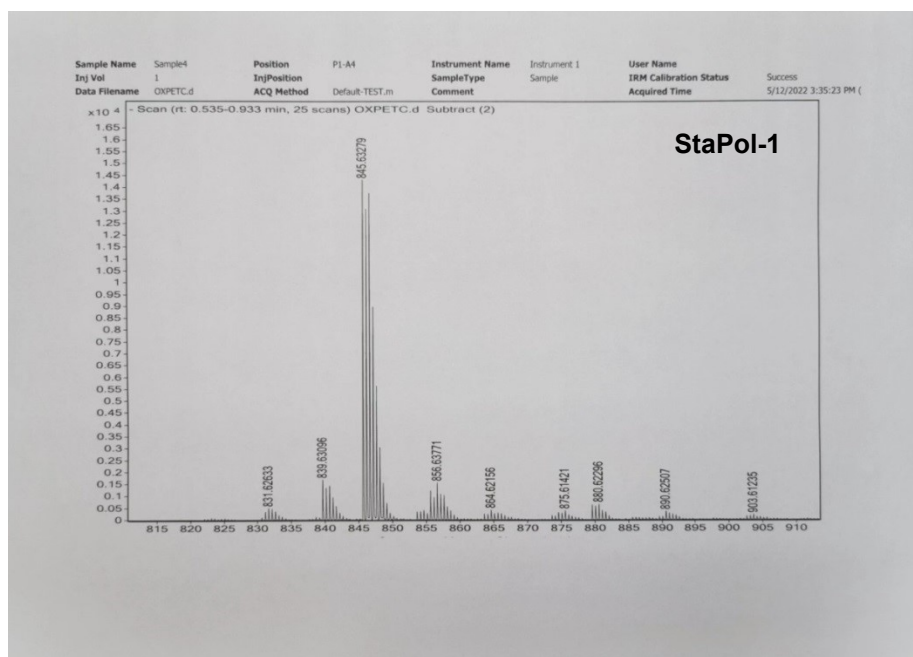


Fig. S9. HRMS spectrum of StaPol-1.

PET #14-21 RT: 0.07-0.10 AV: 8 SB: 23 0.55-0.65 NL: 1.13E9
T: FTMS + p ESI Full ms [100.0000-1500.0000]

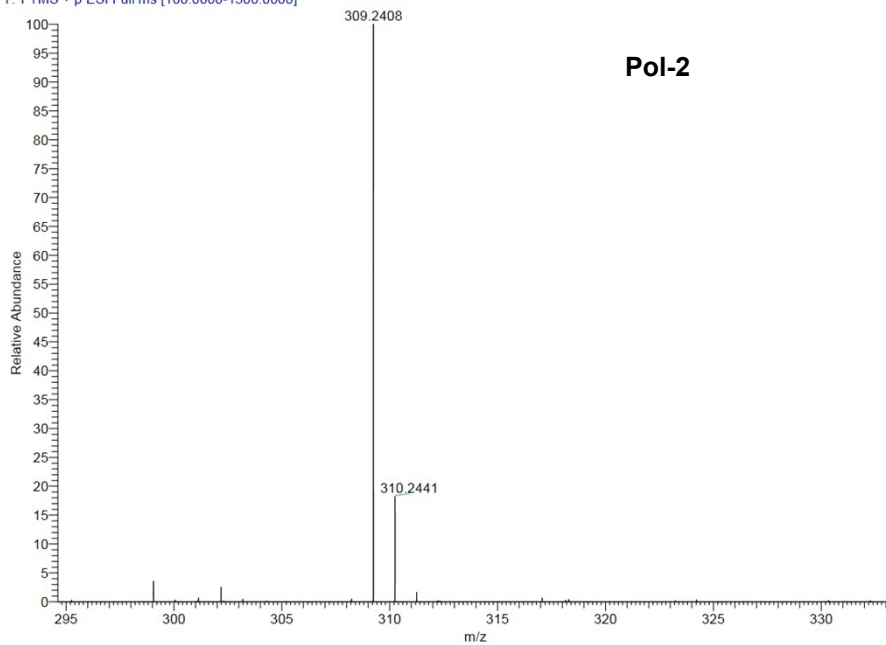


Fig. S10 HRMS spectrum of Pol-2.

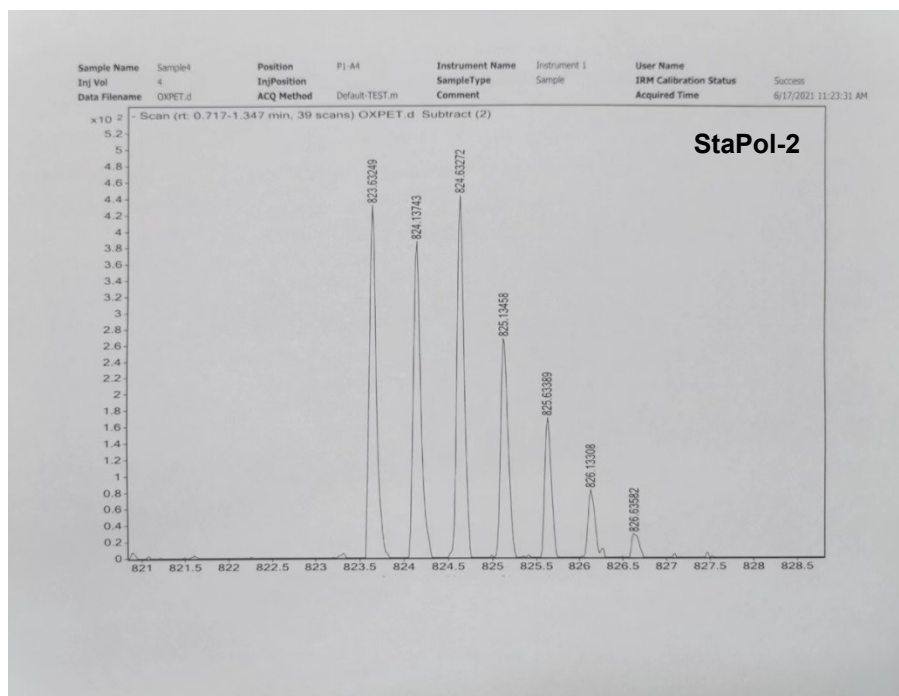


Fig. S11 HRMS spectrum of StaPol-2.

PMT #12-18 RT: 0.06-0.09 AV: 7 NL: 1.20E9
T: FTMS + p ESI Full ms [100.0000-1500.0000]

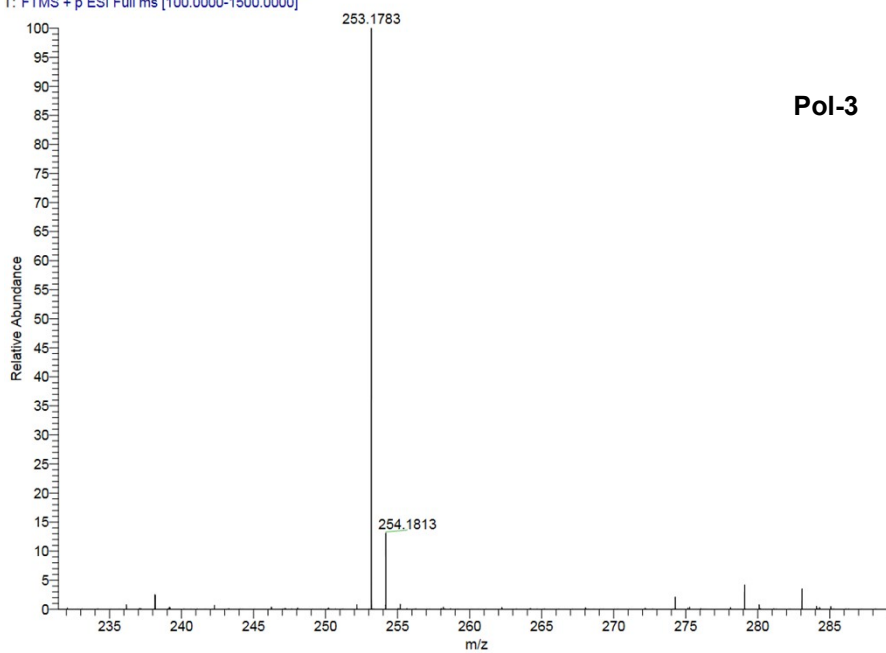


Fig. S12 HRMS spectrum of Pol-3.

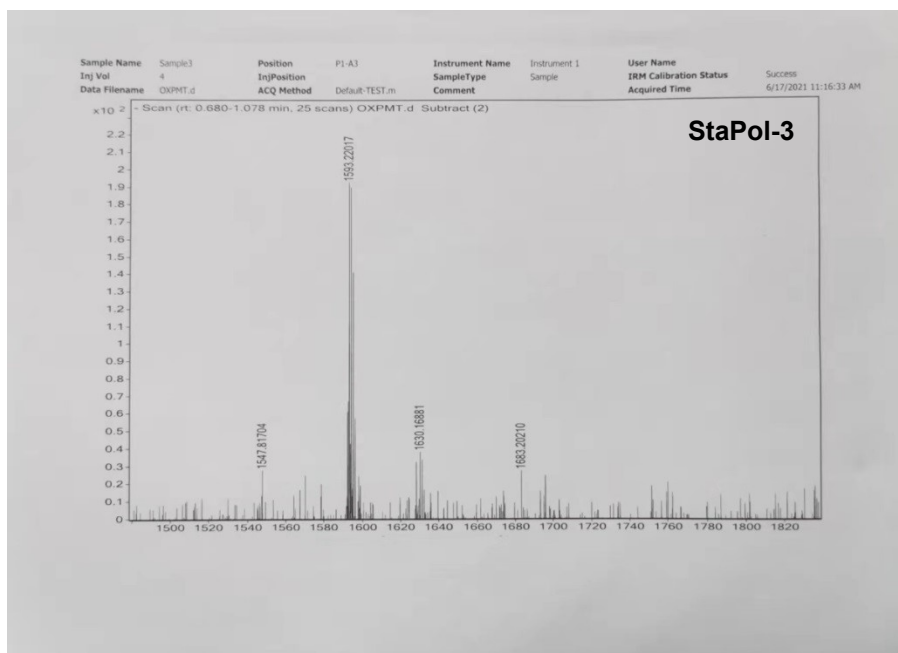


Fig. S13 HRMS spectrum of StaPol-3.

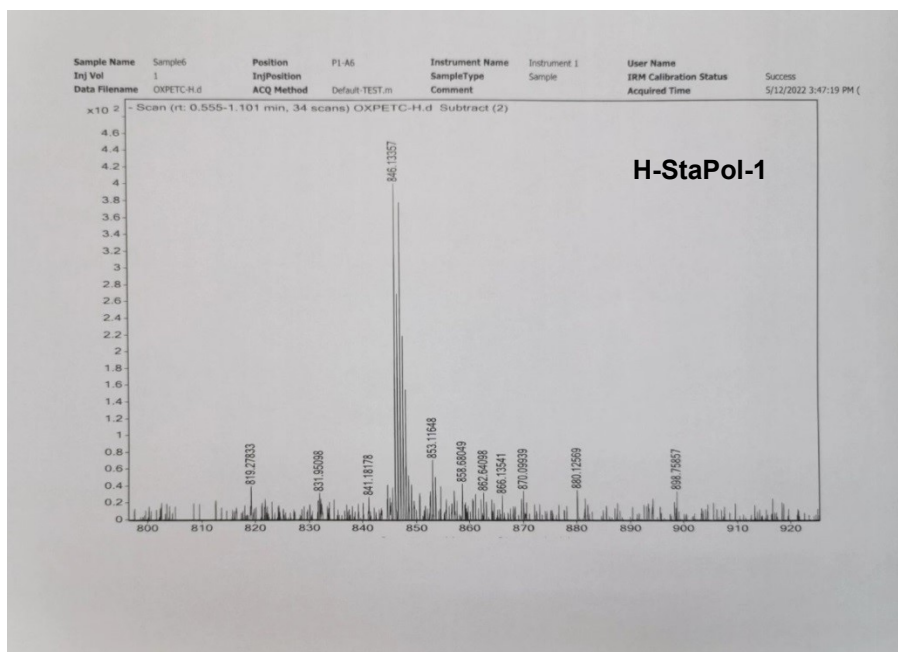


Fig. S14 HRMS spectrum of H-StaPol-1.

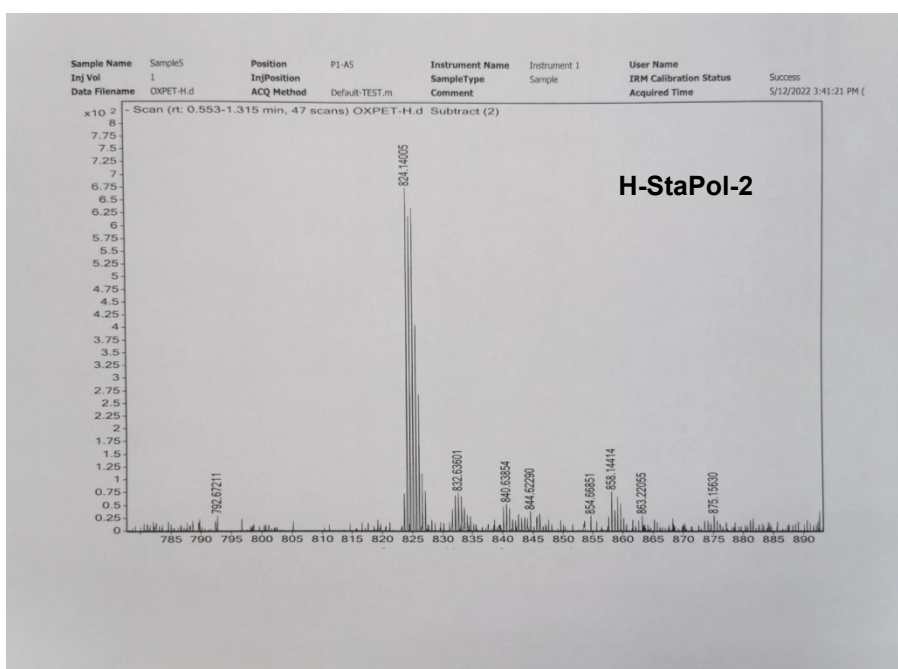


Fig. S15 HRMS spectrum of H-StaPol-2.

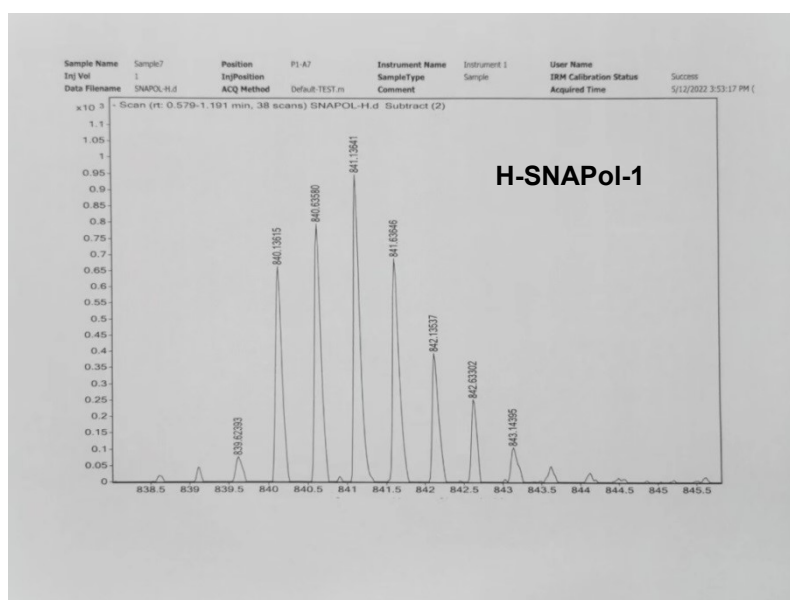


Fig. S16 HRMS spectrum of H-SNAPol-1.

5. Reduction of biradicals with ascorbic acid or in the cell lysates

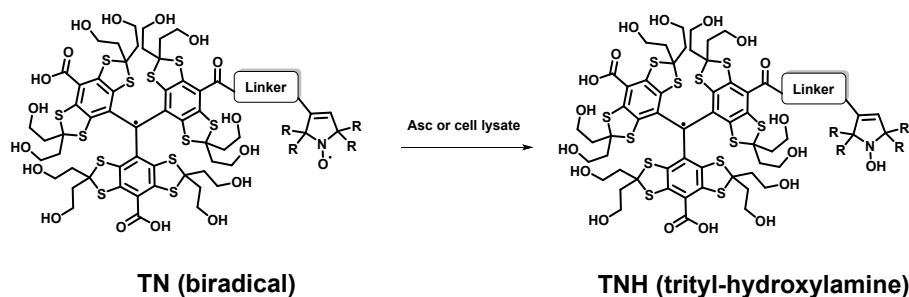


Fig. S17 Reduction of TN biradicals by ascorbic acid or cell lysate.

Assuming that the concentrations of ascorbic acid and reducing substances in cell lysates used were in greater excess than the biradical concentration (50 μM), the reduction of the TN biradical with ascorbic acid or in the cell lysates follows pseudo first-order reaction kinetics. The equations for this reaction kinetics are shown below^{9, 10}:

$$\begin{aligned}
 -\frac{d[TN]}{dt} &= k_2[Asc][TN] \\
 [TN] &= [TN]_0 - [TNH] \\
 k_{obs} &= k_2[Asc] \\
 -\frac{d([TN]_0 - [TNH])}{dt} &= k_2[Asc]([TN]_0 - [TNH]) = k_{obs}([TN]_0 - [TNH]) \\
 \int \frac{d([TN]_0 - [TNH])}{dt} &= \int -k_{obs}([TN]_0 - [TNH]) \\
 \ln\left(\frac{[TN]_0 - [TNH]}{[TN]_0}\right) &= -k_{obs}t
 \end{aligned}$$

where $[TN]$ is the concentration of biradical; k_2 is the second-order rate constant; $[Asc]$ is the ascorbic acid concentration used; $[TN]_0$ is the initial concentration of biradical; $[TNH]$ is the concentration of the trityl-hydroxylamine. The approximated second order rate constant (k_2) was finally calculated from the slope of the plot of k_{obs} versus $[Asc]$. The standard deviation of k_2 was also obtained from the linear fitting of the plots (see the inserted tables in Fig. S21 and S24). Note, the concentration of the trityl radical from the reduction of TN biradicals at different time points were measured based on the signal intensity of the reducing form (i.e., the trityl-hydroxylamine) of StaPol-3 or SNAPol-1 (50 μM) under the same conditions which were obtained by complete reduction with a large excess of ascorbic acid (5 mM) after 30 min.

5. 1. Reduction of biradicals with ascorbic acid

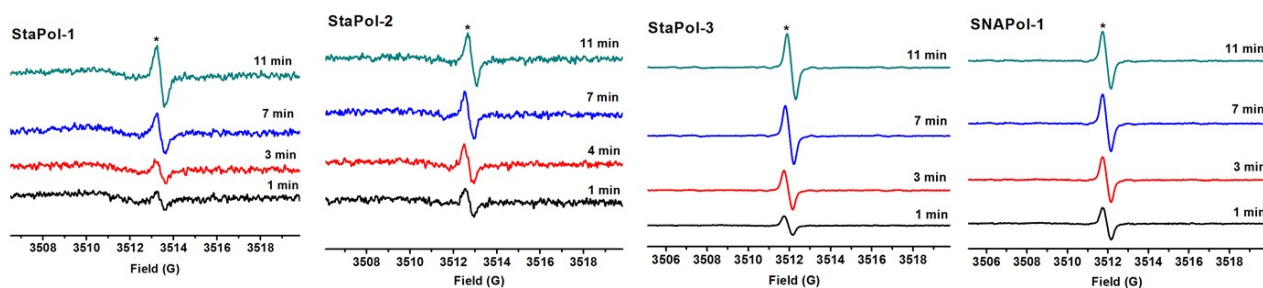


Fig. S18 EPR spectra showing the reactions of StaPol-1, StaPol-2, StaPol-3 or SNAPol-1 (50 μ M) with ascorbic acid (2 mM) in PBS (50 mM, pH 7.4). Spectra were recorded with 100 kHz modulation frequency, 0.8 mW microwave power and 0.1 G modulation amplitude. (Note: In the case of StaPol-1 and StaPol-2, the signal intensity is enlarged for ~ 50 x). The concentrations of the trityl monoradical from reduction of StaPol-1 and StaPol-2 after 11 min were calculated to $2.6 \pm 0.1 \mu$ M and $2.4 \pm 0.1 \mu$ M, implying that only $5.2 \pm 0.2 \%$ and $4.8 \pm 0.2 \%$ of StaPol-1 and StaPol-2 were reduced, respectively.

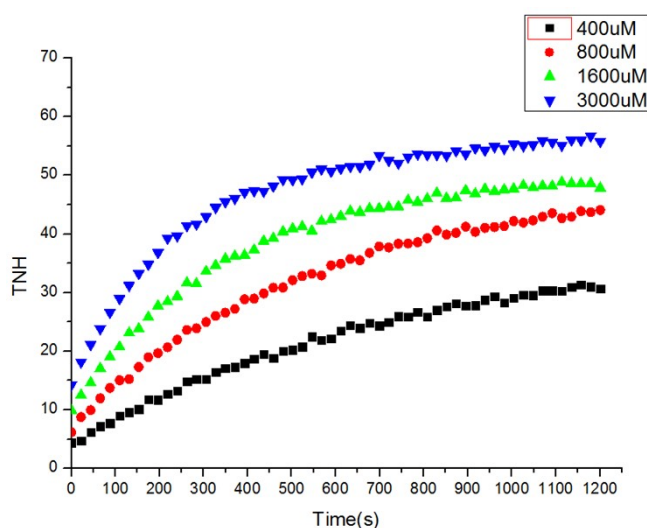


Fig. S19 Plot of concentration of trityl radical as a function of time, which was formed from the reaction of StaPol-3 (60 μ M) with various concentrations of ascorbic acid (400-3000 μ M) in PBS (20 mM, pH 7.4).

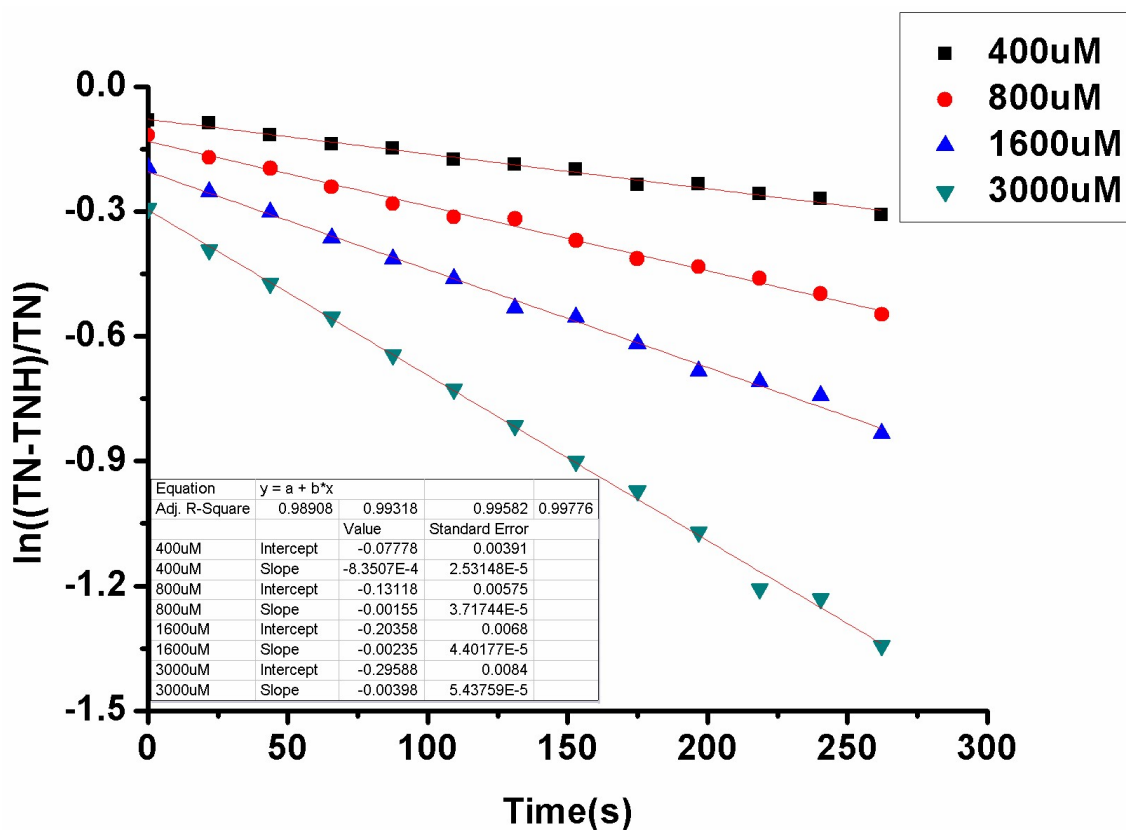


Fig. S20 Plot of $\ln\left(\frac{[TN]_0 - [TNH]}{[TN]_0}\right)$ vs t for StaPol-3.

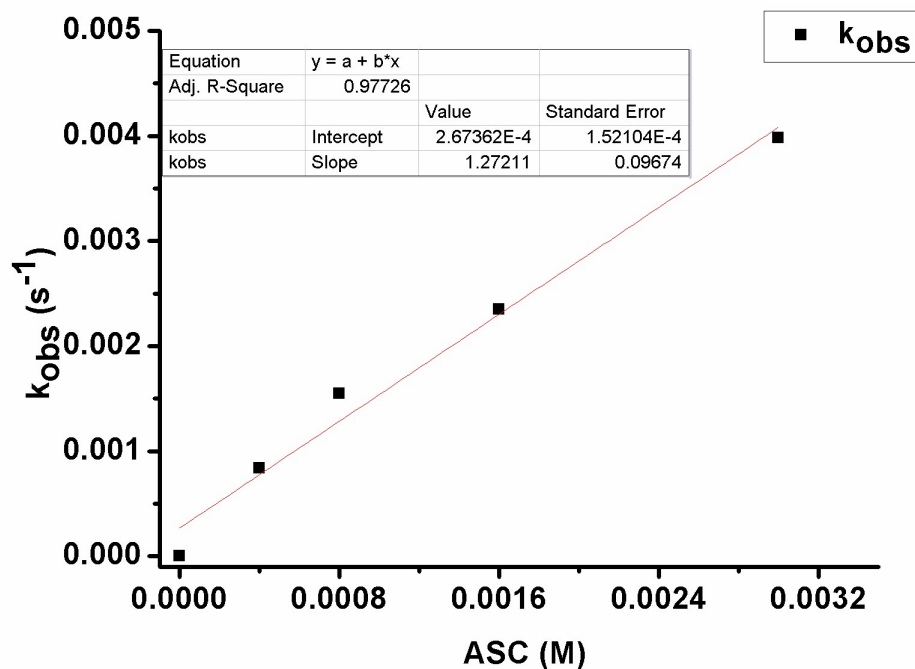


Fig. S21 Plot of k_{obs} vs $[Asc]$ for StaPol-3.

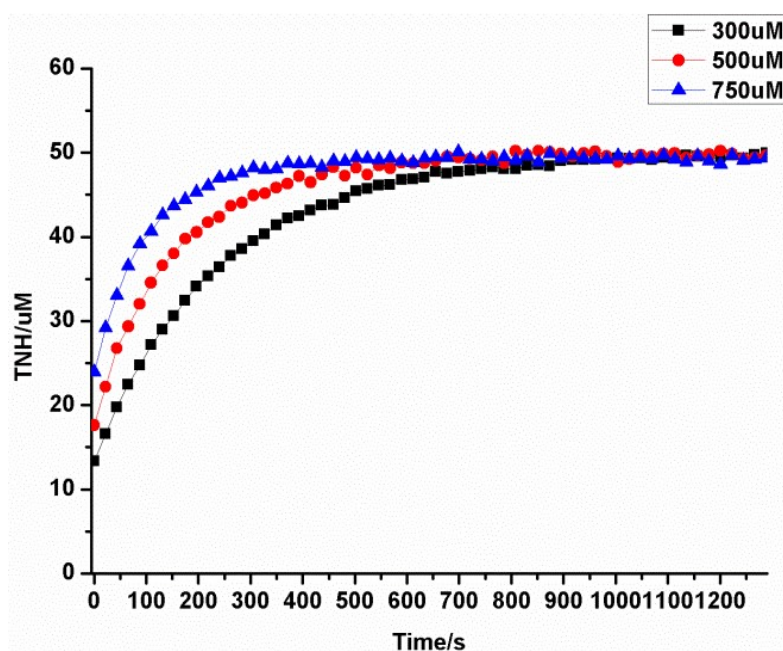


Fig. S22 Plot of concentration of trityl radical as a function of time, which was formed from the reaction of SNAPol-1 (50 μM) with various concentrations of ascorbic acid (300 - 750 μM) in PBS (20 mM, pH 7.4).

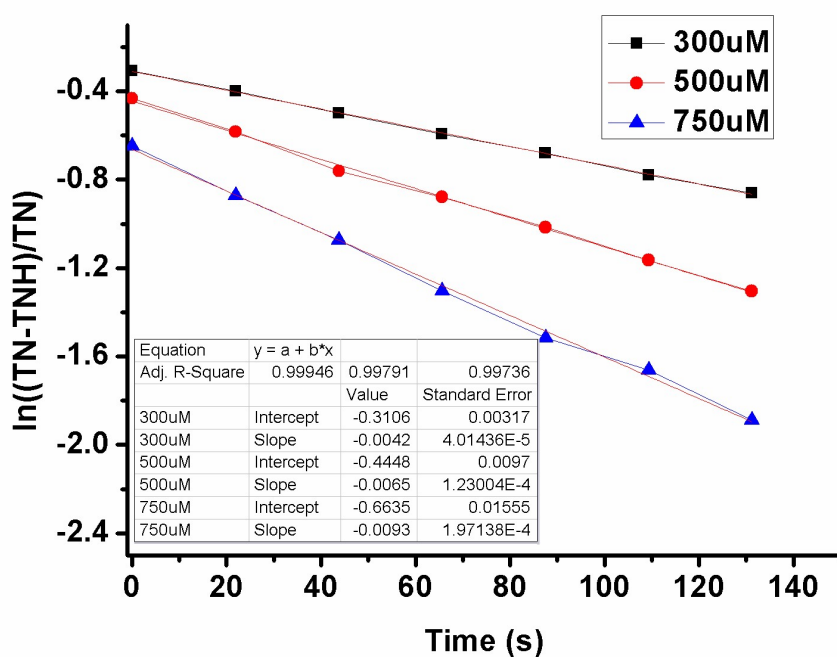


Fig. S23 Plot of $\ln([TN]_0 - [TNH])/[TN]_0$ vs t for SNAPol-1.

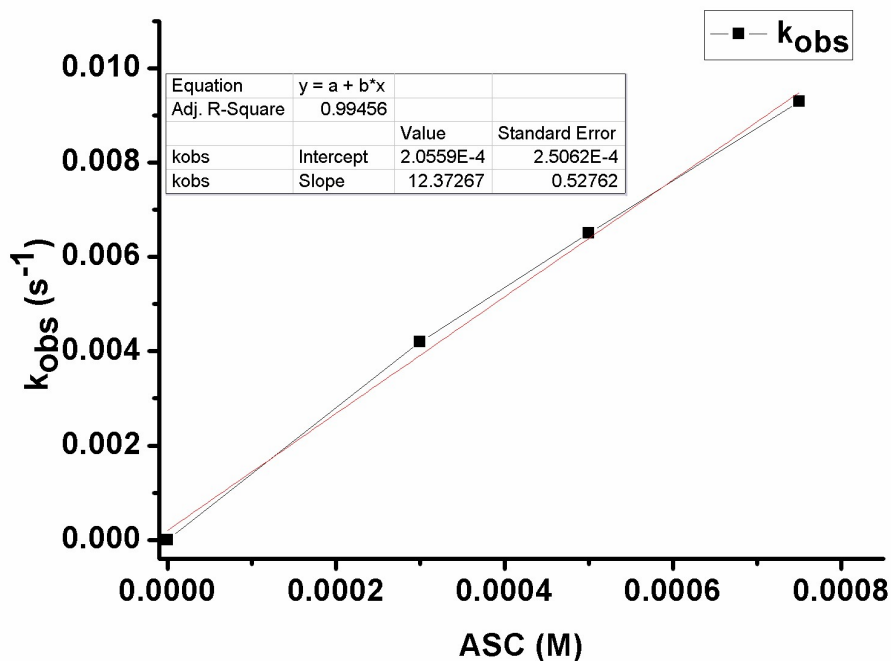


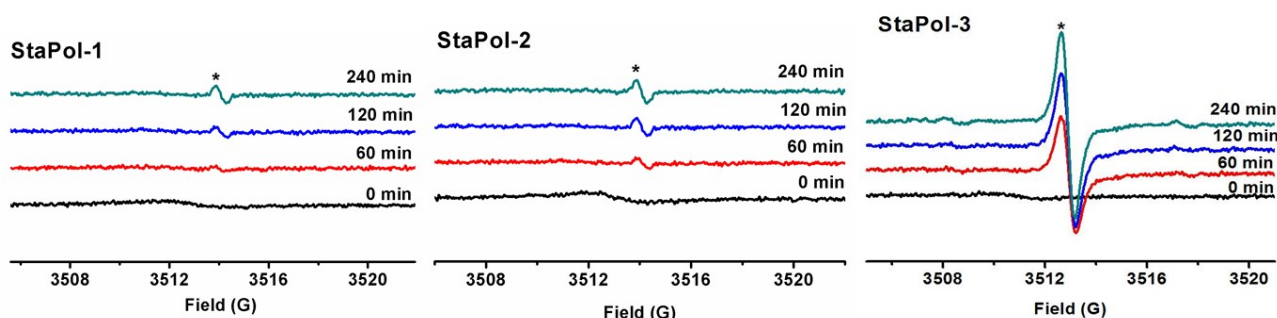
Fig. S24 Plot of k_{obs} vs [Asc] for SNAPol-1.

5.2 Reduction of biradicals in HeLa cell lysates

5.2.1 Preparation of HeLa cell lysates

HeLa cells were cultured in Dulbecco's modified Eagle's medium (DMEM) supplemented with 10% fetal bovine serum (FBS) and 1% penicillin/streptomycin at 37 °C in a humidified atmosphere of 5% CO₂ and 95% air. The cells were used between passages 4 and 6. HeLa cell lysates were prepared according to a reported method with minor modifications.^{11, 12} The HeLa cell suspension (PBS, 600 μ L per 10⁸ cells) was frozen in liquid nitrogen and then thawed in a 37 °C water bath. This procedure was repeated 3 times. The resulting lysate was further sonicated for 5 minutes and then centrifuged at 15000 rpm at 4 °C. The supernatant was taken and stocked at -80 °C.

5.2.2 Stability of biradicals in HeLa cell lysates



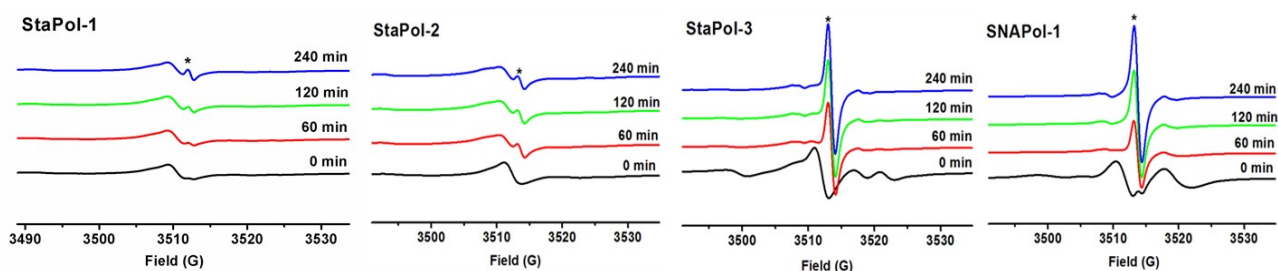


Fig. S25 EPR spectra showing the reduction of StaPol-1, StaPol-2, StaPol-3, and SNAPol-1 in the HeLa cell lysates. The biradical (25 μ L, at the final concentration of 50 μ M) was mixed with HeLa cell lysates (25 μ L) and then EPR spectra were recorded over 240 min. “*” indicates signals from the trityl monoradicals. EPR spectra were recorded with 0.8 mW microwave power and 0.1 G modulation amplitude (top, StaPols), or 10 mW microwave power and 1 G modulation amplitude (bottom, StaPols and SNAPol-1). The concentrations of the trityl monoradical from reduction of StaPol-1 and StaPol-2 after 240-min incubation were calculated to be $1.5 \pm 0.1 \mu\text{M}$ and $1.6 \pm 0.1 \mu\text{M}$, implying that only $3.0 \pm 0.2 \%$ and $3.2 \pm 0.2 \%$ of StaPol-1 and StaPol-2 were reduced, respectively.

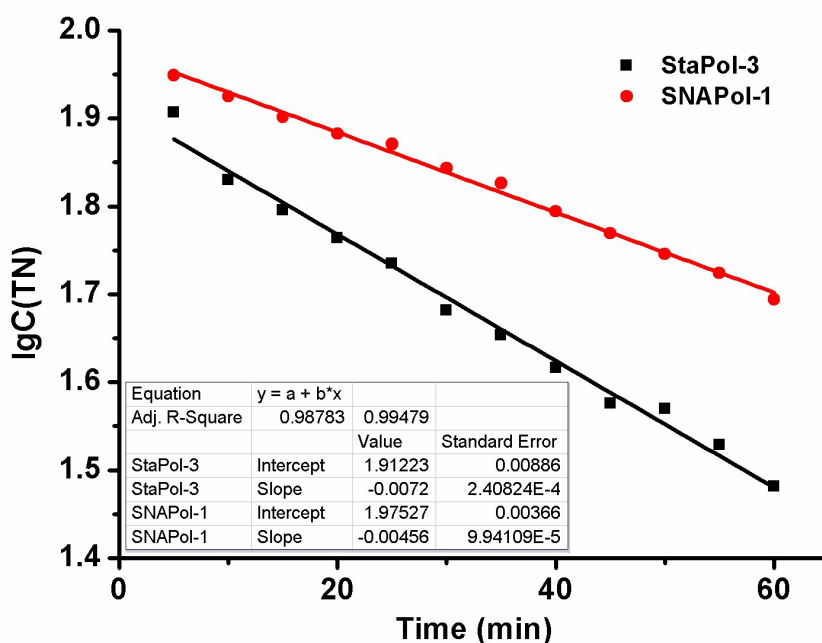


Fig. S26 Plot of $\lg C([TN])$ vs t . Linear fitting provided the value of k from the slope and the corresponding half-lives ($t_{1/2} = \lg 2/k$) of both StaPol-3 and SNAPol-1 in the HeLa cell lysates were obtained.

Table S6. Second-order reaction rates of StaPol-3 and SNAPol-1 with ascorbic acid and half-life times in HeLa cell lysates.

Polarizing Agent	k_2 ($\text{M}^{-1}\text{s}^{-1}$)	$t_{1/2}$ (min)
StaPol-3	1.3 ± 0.1	41.8 ± 1.4
SNAPol-1	12.4 ± 0.5	66.0 ± 1.4

6. Solid-state NMR DNP experiments

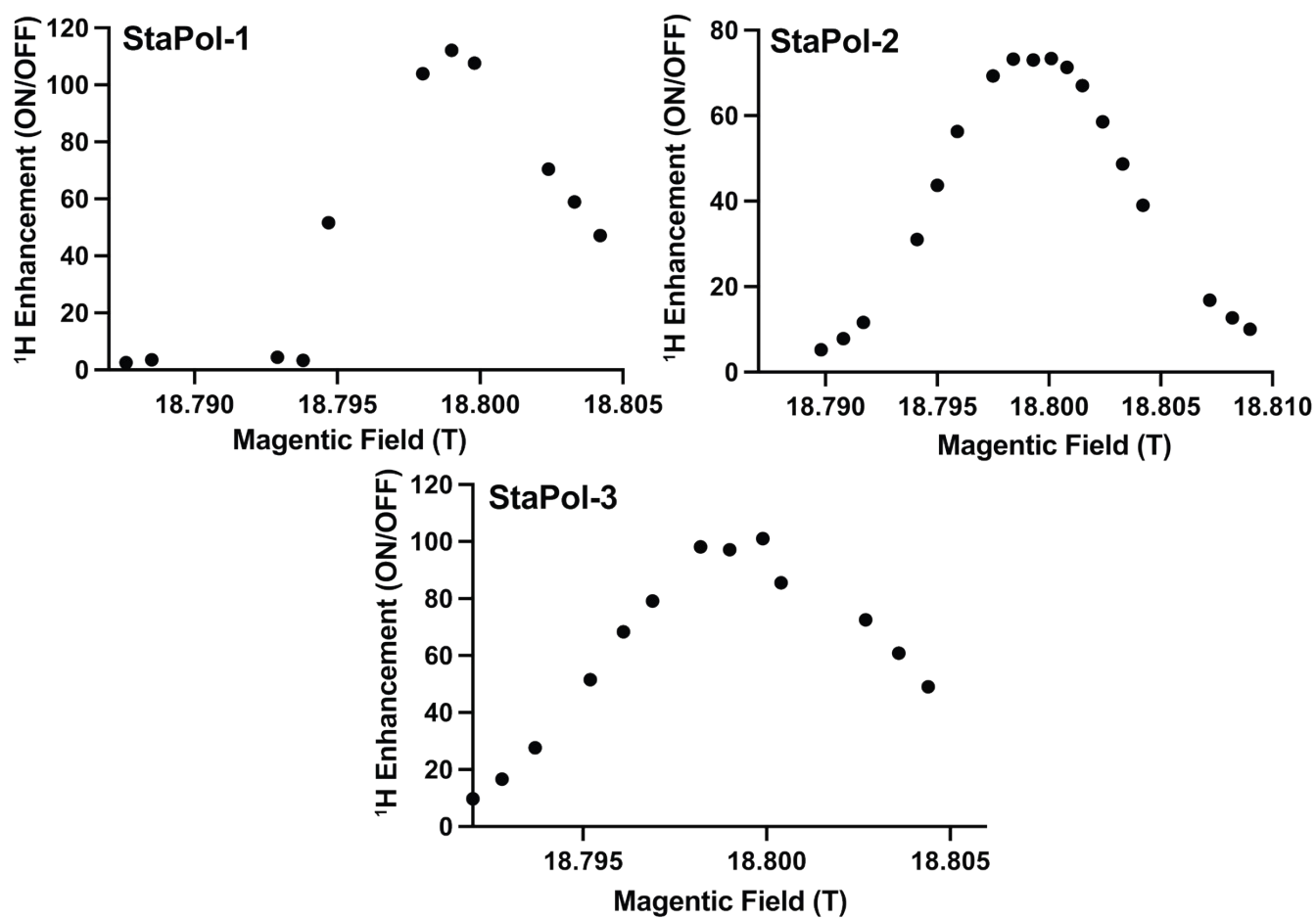
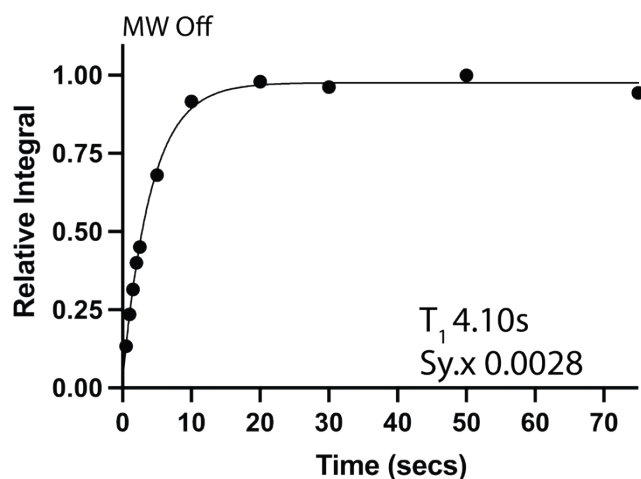
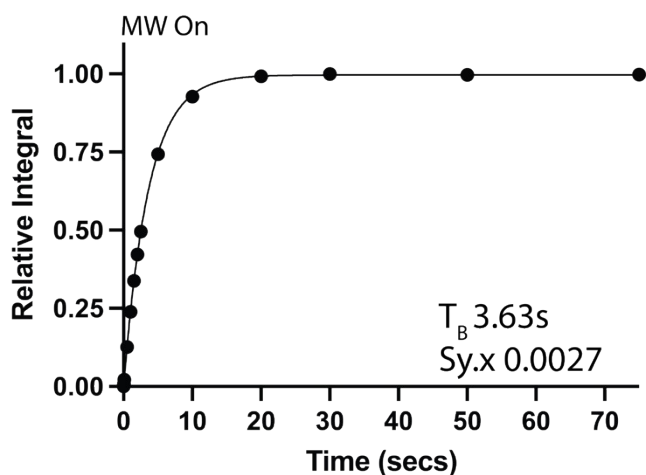
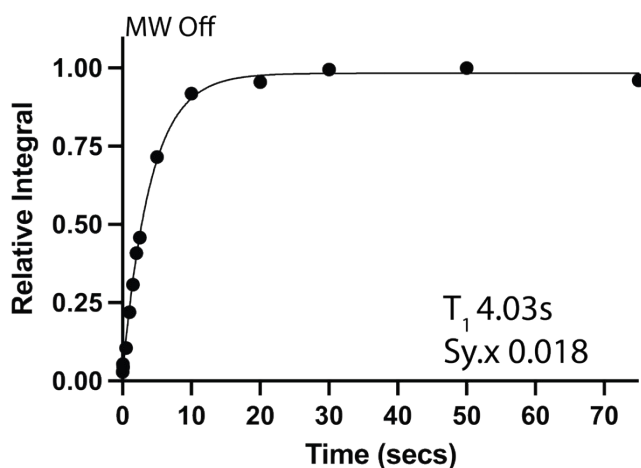
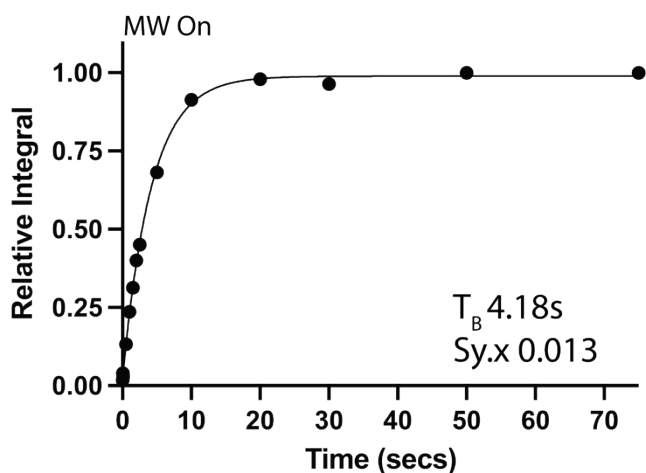


Fig. S27 DNP Field profiles for StaPol-1, StaPol-2, and StaPol-3. PAs were impregnated at a final concentration of 10 mM into a matrix containing 0.25 M [^{13}C , ^{15}N] proline solubilized in the 'DNP Juice' (d_8 -glycerol/ $\text{D}_2\text{O}/\text{H}_2\text{O}$, 60/30/10, v/v/v). See Tables S8-S10 for error analysis.

Stapol-2



StaPol-3



StaPol-1

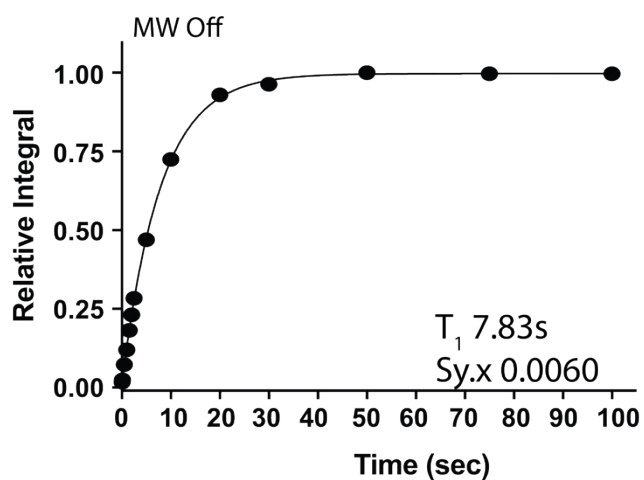
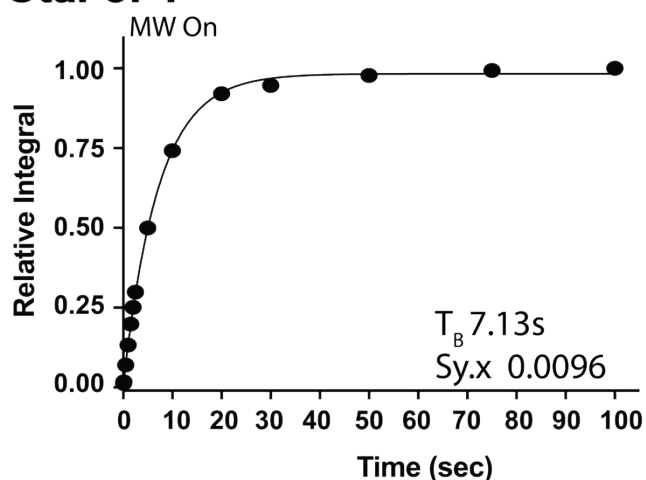


Fig. S28 0.25 M [^{13}C , ^{15}N] proline carbonyl polarization build-up curves for StaPol-2, StaPol-3, and StaPol-1. Left panel depicts T_B (sec) and right panel depicts T_1 (sec). PAs were impregnated at a final concentration of 10 mM into a matrix containing 0.25 M proline solubilized in 'DNP Juice' (d_8 -glycerol/ $\text{D}_2\text{O}/\text{H}_2\text{O}$, 60/30/10, v/v/v). Data is fitted with a mono-exponential decay model. $Sy.x$ denotes the s.d. of the residual. See Tables S11-13 for error analysis.

[¹³C, ¹⁵N] ubiquitin in nuclei
 [¹³C, ¹⁵N] ubiquitin in whole cells
 [¹³C, ¹⁵N] ubiquitin in lysates

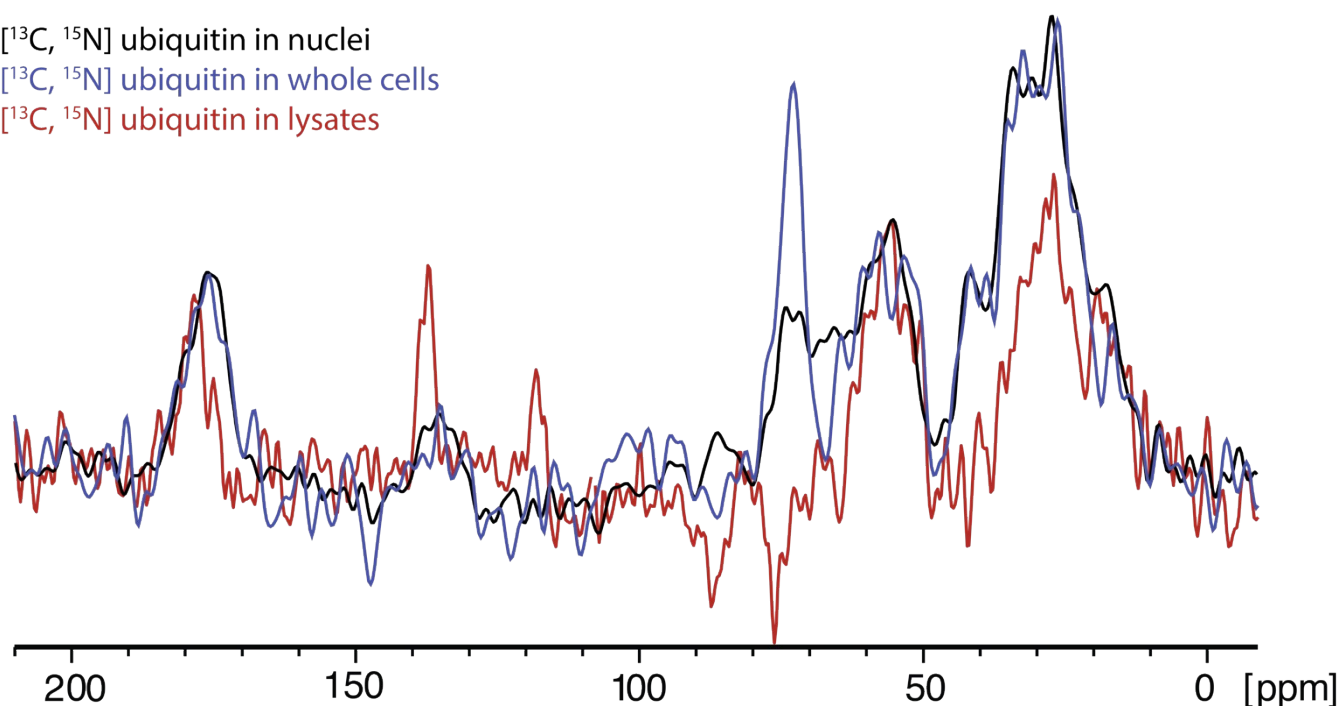


Fig. S29 Comparison of double-quantum ¹³C-¹³C filtered experiments on [¹³C, ¹⁵N] ubiquitin delivered via electroporation to intact HeLa cells (blue), isolated nuclei (black), and lysates (red). Intact HeLa cell and nuclei 1D slices were extracted from 3D DQSQSQ ¹³C-¹³C-¹³C experiments (Berishvili *et al.*, 2022, under review). The overlay shows that the aliphatic resonances observed in lysates most likely stem from labelled ubiquitin with some additional natural abundance signals in the 110 ppm to 150 ppm region. These resonances could result from aromatic Ub residues and/or the natural abundance cellular background including nucleic acids. The increased intensity at 140 ppm is likely due to a superposition of aromatic signals and carbonyl MAS sidebands.

Table S7. Summary of ¹H and ¹³C enhancements for [¹³C, ¹⁵N] proline in ‘DNP juice’ (d₈-glycerol/D₂O/H₂O, 60/30/10, v/v/v). ¹³C enhancements were determined at the magnetic field where maximum ¹H enhancements were detected.

Polarizing Agent	Max ¹ H Enhancement	Max ¹³ C Enhancement
StaPol-1	112 ± 1.3	117 ± 0.90
StaPol-2	73 ± 0.76	84 ± 0.75
StaPol-3	101 ± 0.76	105 ± 1.3
SNAPol-1	/	135

Table S8. Error analysis for the field profile of Stapol-1 in Fig S27. Details of the error calculation are given in the section of solid-state NMR methods.

Stapol-1		
Magnetic Field (T)	Eon/off	Error +/-
18.7876	2.58	1.94
18.7885	3.53	1.71
18.7929	4.41	1.62
18.7938	3.39	1.64
18.7947	51.62	1.50
18.798	103.95	1.23
18.799	112.01	1.27
18.7998	107.66	1.23
18.8024	70.43	1.05
18.8033	58.98	1.05
18.8042	47.15	1.13

Table S9. Error analysis for the field profile of Stapol-2 in Fig S27. Details of the error calculation are given in the section of solid-state NMR methods.

Stapol-2		
Magnetic Field (T)	Eon/off	Error +/-
18.7898	5.25	0.11
18.7908	7.82	0.13
18.7917	11.62	0.16
18.7941	31.03	0.38
18.795	43.69	0.48
18.7959	56.30	0.62
18.7975	69.30	0.73
18.7984	73.26	0.75
18.7993	73.00	0.75
18.8001	73.39	0.76
18.8008	71.31	0.73
18.8015	67.01	0.71
18.8024	58.56	0.65
18.8033	48.72	0.55
18.8042	39.06	0.55
18.8072	16.84	0.21
18.8082	12.73	0.17
18.809	10.01	0.16

Table S10. Error analysis for the field profile of Stapol-3 in Fig S27. Details of the error calculation are given in the section of solid-state NMR methods

Stapol-3		
Magnetic Field (T)	Eon/off	Error +/-
18.792	9.72	0.41
18.7928	16.62	0.52
18.7937	27.60	0.62
18.7952	51.53	1.32
18.7961	68.39	1.16
18.7969	79.17	1.16
18.7982	98.14	0.70
18.799	97.18	0.54
18.7999	101.00	0.76
18.8004	85.60	0.10
18.8027	72.51	1.25
18.8036	60.83	1.28
18.8044	49.08	0.96

Table S11. Error analysis of T_B/T_1 of Stapol-1 from Fig S28. Details of the error calculation are given in the section of solid-state NMR methods.

Stapol-1					
T_B			T_1		
Time (sec)	Relative Integral	Error +/-	Time (sec)	Relative Integral	Error +/-
0.05	0.01257	0.0097	0.05	0.01717	0.0167
0.1	0.0174	0.0011	0.1	0.02452	0.0192
0.5	0.0704	0.0019	0.5	0.07289	0.0517
1	0.1328	0.0019	1	0.1199	0.0547
1.5	0.1986	0.0013	1.5	0.1818	0.0392
2	0.2509	0.0011	2	0.2312	0.0342
2.5	0.2987	0.0027	2.5	0.2835	0.0295
5	0.4998	0.0036	5	0.4695	0.0418
10	0.7417	0.0079	10	0.7248	0.0489
20	0.9206	0.0042	20	0.9295	0.0602
30	0.9463	0.0097	30	0.9633	0.0399
50	0.9775	0.0136	50	1	0.0457
75	0.9932	0.0094	75	0.9967	0.0403
100	1	0.0093	100	0.9967	0.0466

Table S12. Error analysis of T_B/T_1 of Stapol-2 from Fig S28. Details of the error calculation are given in the section of solid-state NMR methods.

Stapol-2					
T_B			T_1		
Time (sec)	Relative Integral	Error +/-	Time (sec)	Relative Integral	Error +/-
0.001	0.0001538	0.0002	0.5	0.1333	0.2515
0.05	0.008734	0.0008	1	0.235	0.1880
0.1	0.02175	0.0008	1.5	0.3151	0.0405
0.5	0.1257	0.0038	2	0.4001	0.0472
1	0.2392	0.0062	2.5	0.4504	0.0419
1.5	0.338	0.0075	5	0.6808	0.0502
2	0.4224	0.0075	10	0.9166	0.0470
2.5	0.4957	0.0057	20	0.9796	0.0438
5	0.7433	0.0082	30	0.9622	0.0448
10	0.9275	0.0094	50	1	0.0424
20	0.9923	0.0100	75	0.9437	0.0465
30	1	0.0096			
50	0.9966	0.0081			
75	0.9978	0.0070			

Table S13. Error analysis of T_B/T_1 of Stapol-3 from Fig S28. Details of the error calculation are given in the section of solid-state NMR methods.

Stapol-3					
T_B			T_1		
Time (sec)	Relative Integral	Error +/-	Time (sec)	Relative Integral	Error +/-
0.001	0.01777	0.0137	0.001	0.02863	0.0278
0.05	0.03997	0.0025	0.05	0.05318	0.0415
0.1	0.02885	0.0008	0.1	0.0442	0.0313
0.5	0.1324	0.0019	0.5	0.1047	0.0478
1	0.2356	0.0015	1	0.2198	0.0474
1.5	0.3128	0.0014	1.5	0.3072	0.0454
2	0.3997	0.0036	2	0.4081	0.0425
2.5	0.4507	0.0033	2.5	0.4582	0.0408
5	0.6812	0.0073	5	0.7151	0.0483
10	0.9137	0.0041	10	0.918	0.0595
20	0.9795	0.0100	20	0.9543	0.0395
30	0.9643	0.0134	30	0.9953	0.0454
50	1	0.0095	50	1	0.0405
75	1	0.0093	75	0.9598	0.0449

Table S14. Error analysis of T_B of Stapol-1 with *in vitro* ^{13}C , ^{15}N ubiquitin in DNP juice (Figure 4b).

T_B		
Time (sec)	Relative Integral	Error +/-
0.5	0.09347	0.0137
1	0.1769	0.0180
1.5	0.2484	0.0046
2	0.3137	0.0020
2.5	0.3708	0.0036
5	0.5939	0.0048
10	0.8338	0.0074
20	0.9664	0.0110
30	0.9843	0.0081
50	0.9805	0.0071
75	0.9885	0.0038
100	1	0.0034

7. Materials and Methods for solid-state NMR DNP experiments

7.1 Production of ^{13}C , ^{15}N -enriched Ubiquitin (Ub)

Stable isotope labelled Ub was produced recombinantly in *E. coli* as described before⁸. Upon purification Ub was buffer exchanged into water and lyophilized for long-term storage. ^1H - ^{15}N SOFAST-HMBC experiments were acquired prior to lyophilization and directly after sample rehydration to ensure Ub's proper fold.

7.2 Production of in-cell samples and lysates

2D HeLa cell cultures were grown as described before. HeLa cells were electroporated with 1.2 mM ^{13}C , ^{15}N -Ub following methodology described in ref.¹³. Lysate samples were prepared as follows: 8 million HeLa cells 5 hr post electroporation, were trypsinized, washed thrice with ice-cold phosphate-buffered saline (PBS - Sigma-Aldrich, Sneldorf-Germany), and centrifuged (400 x g for 3 mins at centigrade). Following aspiration, the white pellet was resuspended on ice in 56 μL of DNP Juice (6:4 - d_8 - $^{12}\text{C}_3$ glycerol: D_2O (1 x Hank's buffered salts) with cell culture protease inhibitors (MERCK, The Netherlands) and passed through a 23 G needle 20 times. The sample was further centrifuged (7,000 x g for 3 mins at 4 centigrade) and the pellet was resuspended by passing through a 23 G needle until the solution was minimally viscous. The samples were split into equal aliquots and supplemented with either SNAPol-1 or StaPol-1 at a final concentration of 30 mM. The aliquots were incubated at ambient temperature for 1.5 hrs and then packed into DNP sapphire 3.2 mm rotors as described in ref.^{13, 14}.

7.3 Acquisition of DNP-ssNMR Data

All data were acquired at a static magnetic field strength of 18.8 T - ^1H 800 MHz. The spectrometer was equipped with an AVANCE NEO console (Bruker Corp, USA), 3.2 mm HX low-temperature DNP probe, sweep coil, and a 9.7 T - 527 GHz gyrotron. All measurements were conducted at a MAS rate of 8 kHz and 95K. Spectra requiring proton-decoupling utilized SPINAL-64¹⁵ at a strength of 85 kHz. Data was collected at 60 mA of microwave irradiation.

7.4 Enhancement Field Profiles

All PAs (30 mM) were impregnated into a matrix consisting of 0.25 M ^{13}C , ^{15}N proline dissolved in 6:3:1 DNP Juice (d_8 -glycerol/ D_2O / H_2O), placed into sapphire DNP rotors and flash frozen in liquid nitrogen. PA field profiles were recorded for ^1H at various magnetic fields utilizing a Hahn-echo pulse sequence¹⁶ - ^{13}C enhancements were determined indirectly via a ^1H - ^{13}C at the field strength where maximum ^1H enhancement was recorded. Specific experimental parameters can be found in Table S7.

7.5 T_1 and T_B Measurements and Enhancements

Relaxation measurements were obtained via a saturation recovery adiabatic ^1H - ^{13}C CP.⁸ Experimental parameters as listed above. Relaxation data was fit in Prism with the following formula:

$$I[t] = I[0] \left(1 - e^{-t/T_1} \right)$$

7.6 Error Analysis

The enhancement error ($\Delta\epsilon$) was calculated as described in Ref. [17, 18] according to the following formula:

$$\Delta\epsilon = \epsilon (\Delta I_{\mu\text{w,on}}/I_{\mu\text{w,on}} + \Delta I_{\mu\text{w,off}}/I_{\mu\text{w,off}})$$

where I is the intensity and ΔI is the signal to noise in DNP experiments with and without microwaves on.

For T_1 and T_B buildup curves, the error is reported as standard deviation (s.d.) of the signal to noise (S/N). The S/N was determined using the following formula:

$$\text{signal to noise} = \frac{\text{maxval}}{2 \cdot \text{noise}}$$
$$\text{noise} = \sqrt{\frac{\sum_{i=-n}^n y(i)^2 - \frac{1}{n} \left(\sum_{i=-n}^n y(i) \right)^2 + \frac{3 \cdot \left(\sum_{i=-n}^n i(y(i) - y(-i))^2 \right)}{N^2 - 1}}{N - 1}}$$

where *maxval* is the highest intensity within the designated region, N is the total number of points within the noise,

$n = \frac{(N-1)}{2}$, and $y(i)$ in the n th point in the noise region – adapted Bruker Topspin 4.1.1.

$S_{y,x}$ denotes the standard deviation of the residuals. It is computed as follows:

$$S_{y,x} = \sqrt{\frac{\sum (\text{residual}^2)}{n - K}}$$

where $n-k$ is the degrees of freedom of the regression – adapted from PRISM.

7.7 2D ^{13}C - ^{13}C PDSO

PDSO experiments were acquired with a 30 ms spin diffusion time (see ,e.g. Ref.¹⁹). The carrier frequency was placed at 75 ppm. *In vitro* spectra were acquired with 656 points in the indirect dimension and 2368 points in the direct dimension. Lysate StaPol-1 spectra were acquired with 328 points in the indirect dimension and 2368 points in the direct dimension. Data was processed in Topspin 4.1.1 with qsine SSB 2 for all spectral dimensions.

7.8 1D ^{13}C - ^{13}C 2Q-1Q

1D ^{13}C - ^{13}C double quantum experiments utilized a 0.5 msec reconversion to suppress DNP juice depleted glycerol signals.¹³ ¹⁴ ^1H - ^{13}C asymmetric CP with a 110 μsec contact time (63 kHz ^1H and 72 kHz ^{13}C) was used. Double quantum reconversion was achieved by utilizing 10 spc5²⁰ blocks (0.5 msec total mixing time at ^{13}C 40 kHz) with continuous ^1H decoupling at 90 kHz. The StaPol-1 lysate spectra were acquired with 1132 points, 1792 scans, 64 step phase cycle, recycle delay of 2 secs, and an acquisition time of 7.92 msec.

Table S15. Acquisition parameters for MW ON 1D ^1H - ^{13}C CP experiments. MW OFF experiments utilized identical parameters but with the MW source off. The StaPol-1 - ^{13}C , ^{15}N Ub in-cell DQSQ was recorded with both 512 and 2048 scans, the latter was utilized for analysis but baseline imperfections were still prominent.

	StaPol-1 - ^{13}C , ^{15}N Ub	StaPol-1 - ^{13}C , ^{15}N Ub in-cell	SNAPol-1 - ^{13}C , ^{15}N Ub lysates	StaPol-1 - ^{13}C , ^{15}N Ub lysates
^1H 90 (μs)	3.25	2.25	3	3
^{13}C 90 (μs)	2.75	2.75	3.25	5.2
CP Contact Time (μs)	700	110	200	200
Acquisition Time (ms)	4.5	4.5	8.9	8.9
Line broadening (Hz)	100	200	100	100
Number of Scans	128	512	2048	2048

Table S16. Acquisition parameters for 2D ^{13}C - ^{13}C PDSO experiments. Experiment utilized 90 pulse lengths as listed in Table S8.

	StaPol-1 - ^{13}C , ^{15}N Ub
Acquisition Time (ms) F2: F1	14.5/4.1
NS	64
Recycle delay	2
Line broadening (Hz)	125

References

1. H. Wu, V. Coble, O. Vasalatiy, R. E. Swenson, M. C. Krishna and J. B. Mitchell, *Tetrahedron Lett.*, 2014, **55**, 5570-5571.
2. Y. Wang, J. T. Paletta, K. Berg, E. Reinhart, S. Rajca and A. Rajca, *Org. Lett.*, 2014, **16**, 5298-5300.
3. M. Ponceleta, J. L. Huffmana, V. V. Khramtsov, I. Dhimitrukad and B. Driesschaert, *RSC Adv.*, 2019, **9**, 35073-35076.
4. W. Moore, R. Yao, Y. P. Liu, S. S. Eaton and G. R. Eaton, *J. Magn. Reson.*, 2021, **332**, 107078.
5. Y. P. Liu, F. A. Villamena, A. Rockenbauer, Y. G. Song and J. L. Zweier, *J. Am. Chem. Soc.*, 2013, **135**, 2350-2356.
6. G. Karthikeyan, A. Bonucci, G. Casano, G. Gerbaud, S. Abel, V. Thome, L. Kodjabachian, A. Magalon, B. Guigliarelli, V. Belle, O. Ouari and E. Mileo, *Angew. Chem. Int. Ed. Engl.*, 2018, **57**, 1366-1370.
7. S. R. Burks, M. A. Makowsky, Z. A. Yaffe, C. Hoggie, P. Tsai, S. Muralidharan, M. K. Bowman, J. P. Kao and G. M. Rosen, *J. Org. Chem.*, 2010, **75**, 4737-4741.
8. X. Y. Cai, A. L. Paioni, A. Adler, R. Yao, W. X. Zhang, D. Beriashvili, A. Safeer, A. Gurinov, A. Rockenbauer, Y. G. Song, M. Baldus and Y. P. Liu, *Chem. Eur. J.*, 2021, **27**, 12758-12762.
9. Y. P. Liu, F. A. Villamena, A. Rockenbauer and J. L. Zweier, *Chem. Comm.*, 2010, **46**, 628-630.
10. Y. P. Liu, F. A. Villamena, Y. G. Song, J. Sun, A. Rockenbauer and J. L. Zweier, *J. Org. Chem.*, 2010, **75**, 7796-7802.
11. N. Fleck, C. Heubach, T. Hett, S. Spicher, S. Grimme and O. Schiemann, *Chem. Eur. J.*, 2021, **27**, 5292-5297.
12. N. Fleck, C. A. Heubach, T. Hett, F. R. Haege, P. P. Bawol, H. Baltruschat and O. Schiemann, *Angew. Chem. Int. Ed.*, 2020, **59**, 9767-9772.
13. S. Narasimhan, S. Scherpe, A. L. Paioni, J. van der Zwan, G. E. Folkers, H. Ovaa and M. Baldus, *Angew. Chem. Int. Ed.*, 2019, **58**, 12969-12973.
14. S. Narasimhan, C. Pinto, A. L. Paioni, J. van der Zwan, G. E. Folkers and M. Baldus, *Nat. Protoc.*, 2021, **16**, 893-918.
15. B. M. Fung, A. K. Khitrin and K. Ermolaev, *J. Magn. Reson.*, 2000, **142**, 97-101.
16. A. Gurinov, B. Sieland, A. Kuzhelev, H. Elgabarty, T. D. Kuhne, T. Prisner, J. Paradies, M. Baldus, K. L. Ivanov and S. Pylaeva, *Angew. Chem. Int. Ed.*, 2021, **60**, 15371-15375.
17. W. X. Zhai, A. L. Paioni, X. Y. Cai, S. Narasimhan, J. Medeiros-Silva, W. X. Zhang, A. Rockenbauer, M. Weingarh, Y. G. Song, M. Baldus and Y. P. Liu, *J. Phys. Chem. B.*, 2020, **124**, 9047-9060.
18. M. Lelli, S. R. Chaudhari, D. Gajan, G. Casano, A. J. Rossini, O. Ouari, P. Tordo, A. Lesage and L. Emsley, *J. Am. Chem. Soc.*, 2015, **137**, 14558-14561.
19. M. Renault, M. P. Bos, J. Tommassen and M. Baldus, *J. Am. Chem. Soc.*, 2011, **133**, 4175-4177.
20. M. Hohwy, C. M. Rienstra, C. P. Jaroniec and R. G. Griffin, *J. Chem. Phys.*, 1999, **110**, 7983-7992.